Phospholipase A_2 Engineering. The Structural and Functional Roles of Aromaticity and Hydrophobicity in the Conserved Phenylalanine-22 and Phenylalanine-106 Aromatic Sandwich†

Cynthia M. Dupureur,‡,§ Bao-Zhu Yu,‖ J. Anthony Mamone,‡,⊥ Mahendra K. Jain,*,‖ and Ming-Daw Tsai*,‡

Department of Chemistry, The Ohio State University, Columbus, Ohio 43210, and Department of Chemistry and Biochemistry, University of Delaware, Newark, Delaware 19716

Received May 1, 1992; Revised Manuscript Received August 11, 1992

ABSTRACT: The highly conserved phenylalanine-22 and phenylalanine-106, arranged as an aromatic sandwich, form part of an invariant hydrophobic wall that shields the active site of bovine pancreatic phospholipase A_2 (PLA2) from bulk solvent [Dijkstra, B. W., Drenth, J., & Kalk, K. H. (1981) *Nature 289*, 604–606]. The residues have also been suggested to interact with the *sn*-2 acyl chain of bound phospholipid substrate [White, S. P., Scott, D. L., Otwinowski, Z., Gelb, M. H., & Sigler, P. B. (1990) *Science 250*, 1560–1563]. We now report the importance of these two residues in the structure and function of PLA2 in terms of aromaticity (changing to Ile) and hydrophobic (changing to Ala) and hydrophilic (changing to Tyr) character of these residues. The structural properties of the mutants were analyzed by proton NMR and by guanidine hydrochloride-induced denaturation. The functional properties were determined by measuring kinetic parameters toward various substrates in the forms of monomers, micelles, and vesicles, and by measuring equilibrium dissociation constants at the interface. The results show that (i) The conformational stability of each mutant was as good as that of wild-type PLA2; none of the mutants was significantly perturbed structurally as judged from detailed ^{1}H NMR analysis. These results suggest that neither the Phe-22/Phe-106 face-to-face pair nor the Phe-22/Tyr-111 edge-to-face pair plays a significant structural role. (ii) Mutations to Ile at either position 22 or position 106 resulted in only minor perturbations in activity. This suggests that the aromaticity is not important to the function of these two residues. (iii) Substitution at either of these two positions with Ala resulted in 10–200-fold decreases in catalytic activities, suggesting that the hydrophobic bulk of both residues is important for catalysis, possibly by interacting with the *sn*-2 acyl chain. (iv) Replacement of Phe-106 by Tyr resulted in decreased activity; the same substitution at position 22 produced an enzyme with wild-type activity. The differential behavior of the two mutants can be rationalized by the orientation of the side chains: Phe-22 points outward facing solvent, whereas Phe-106 points into the active site. (v) Detailed analysis of all the mutants using scooting mode kinetics and equilibrium measurements suggested that the perturbation in the function of F22A, F106A, and F106Y lies primarily in k_{cat}; binding of the enzyme to the interface and binding of ligands to the enzyme at the interface are less perturbed.

The structure of phospholipase A_2 (PLA2)[1] is characterized by a large number of disulfide bonds (seven in a molecular weight of 14 000 for pancreatic PLA2), an extensive hydrogen-bonding network at the active site, and a few aromatic–aromatic pairs surrounding the active site. In this study, we extend our structure–function studies of PLA2 with an exploration of the conserved aromatic pair composed of Phe-22 and Phe-106. These residues first gained attention with the report of the crystal structure of the bovine enzyme (Dijkstra et al., 1981a,b), where it was noted that the core of the active site was shielded by a highly invariant "hydrophobic wall" composed of residues Ile-9, Ala-102, Ala-103, Phe-22, and Phe-106 (Figure 1). As shown in Figure 1, the hydrophobic interactions further extend to Phe-5, Leu-41, and Tyr-111. Two of the residues involved in this hydrophobic network, Phe-5 and Ile-9, have been suggested to be part of a "hydrophobic channel" critical to binding of substrates in interfacial catalysis by PLA2 (White et al., 1990).

The potential structural roles of the Phe-22/Phe-106 aromatic pair are interesting. There is growing evidence that many conserved aromatic residues participate in a variety of interactions that can contribute to enzyme structure and stability (Burley & Petsko, 1985, 1988; Serrano et al., 1991). The near-parallel geometry of Phe-22 and Phe-106 is uncommon and is expected to contribute very little stabilization

† This work was supported by Research Grants GM41788 (to M.-D.T.) and GM29703 (to M.K.J.) from National Institutes of Health and by a National Need fellowship to C.M.D. This is paper no. 9 in the series *Phospholipase A_2 Engineering*. For paper no. 8, see Sekharudu et al. (1992).

‡ The Ohio State University; M.-D.T. is also a member of the Department of Biochemistry.

§ Current address: Department of Chemistry, California Institute of Technology, Pasadena, CA 91125.

‖ University of Delaware.

⊥ Current address: United States Biochemical, Cleveland, OH 44122.

[1] Abbreviations: CD, circular dichroism; COSY, correlated spectroscopy; 1D, one dimensional; 2D, two dimensional; DC_6PC, 1,2-dihexanoyl-*sn*-glycero-3-phosphocholine; DC_7PC, 1,2-diheptanoyl-*sn*-glycero-3-phosphocholine; DC_8PC, 1,2-dioctanoyl-*sn*-glycero-3-phosphocholine; DC_8PM, 1,2-dioctanoyl-*sn*-glycero-3-phosphomethanol; DC_{14}-PM, 1,2-dimyristoyl-*sn*-glycero-3-phosphomethanol; deoxy-LPC, 1-hexadecylpropanediol-3-phosphocholine; DTPC, 1,2-ditetradecyl-*sn*-glycero-3-phosphocholine; DTPM, 1,2-ditetradecyl-*sn*-glycero-3-phosphomethanol; EDTA, ethylenediaminetetraacetate; GdnHCl, guanidine hydrochloride; HDNS, dansylated hexadecylphosphoethanolamine; MJ33, 1-hexadecyl-3-trifluoroethyl-*sn*-glycero-2-phosphomethanol; NOE, nuclear Overhauser effect; NOESY, nuclear Overhauser enhancement spectroscopy; pH*, pH in D_2O without correcting for the deuterium effect. PLA2, phospholipase A_2; WT, wild type.

0006-2960/92/0431-10576$03.00/0

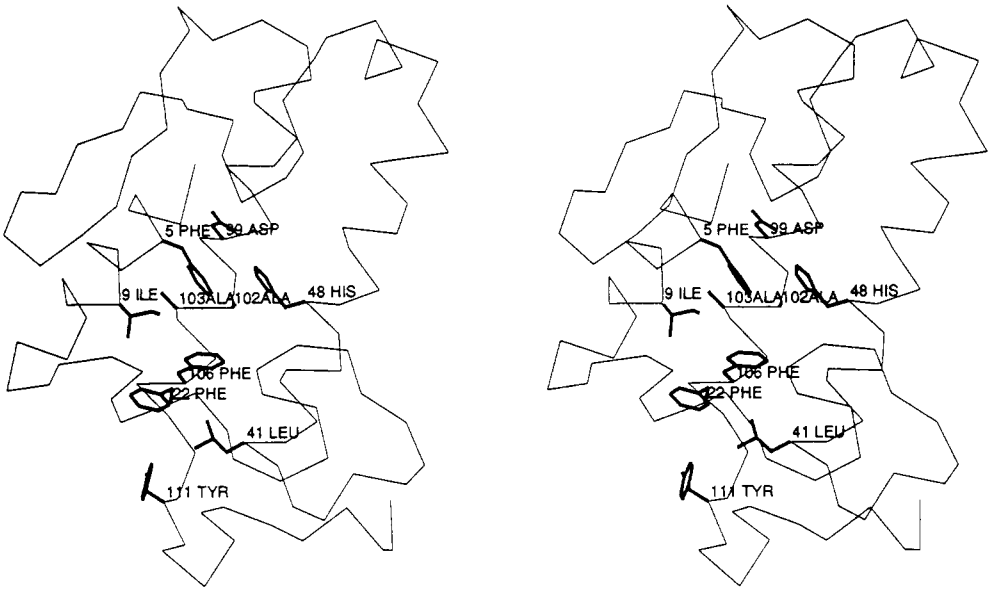

FIGURE 1: Stereogram of the α-carbon traces of bovine pancreatic PLA2 from the 1.8-Å crystal structure (Noel et al., 1991), with the side chains of pertinent residues highlighted.

energy (Singh & Thornton, 1985; Burley & Petsko, 1985). However, to date no experimental evidence has been reported which supports this prediction. Furthermore, Phe-22 is further involved in an edge-to-face interaction with Tyr-111, which can contribute 1.5 kcal/mol of stabilization (Burley & Petsko, 1988; Serrano et al., 1991). To assess the possible structural roles of Phe-22 and Phe-106, we evaluated a number of PLA2s mutated at these positions by measuring their conformational stabilities and performing 1D and 2D ^1H NMR analyses.

Information regarding possible functional roles for Phe-22 and Phe-106 developed a few years ago when we coupled crystallographic information to bioorganic studies to propose one of the first enzyme–substrate binding models for PLA2 (Rosario-Jansen et al., 1987). In this model, we suggested that the catalytically required Ca(II) coordinates with the *pro-S* oxygen of the phosphate and that Tyr-69 forms a hydrogen bond with the *pro-R* oxygen of the phosphate; we also positioned the 2-acyl chain of the substrate near the highly conserved, antiparallel aromatic sandwich formed by Phe-22 and Phe-106. Recently published structures of the crystals of PLA2·transition-state analogue complexes have confirmed the first two features and also demonstrated the proximity of the 2-acyl chain of the substrate to Phe-22 and Phe-106 (White et al., 1990; Scott et al., 1990; Thunnissen et al., 1990). This is further substantiated by the structural information obtained in solution: Phe-22 and Phe-106 are among those residues whose signature NMR properties are perturbed upon both monomeric and aggregated substrate binding (Dekker et al., 1991a).

While such structural studies have provided us with valuable information about enzyme–substrate interactions, they by their nature do not provide us with information regarding the *strength and importance* of these interactions for the function of the enzyme. Using a multifaceted approach involving extensive kinetic and functional characterization of site-directed mutants, as well as structural characterization by ^1H NMR, we address these structure–function questions.

Two major conclusions have been reached: (i) the side chain of neither residue contributes to the stability or the global conformation of the enzyme; (ii) the size and hydrophobicity, but not the aromaticity of the two side chains, contribute modestly to the activity.

MATERIALS AND METHODS

Materials and Routine Procedures. Oligonucleotides were obtained from the Biochemical Instrument Center at the Ohio State University. The following lipids used in this study were prepared as described previously: DTPM (Jain et al., 1986a); $DC_{14}PM$ (Jain & Gelb, 1991); HDNS (Jain & Vaz, 1987); MJ33 (Jain et al., 1991d). All other phospholipid substrates were purchased from Avanti Polar Lipids (Birmingham, AL). Ultrapure guanidine hydrochloride was purchased from ICN Biomedicals. 99.96 atom % D D_2O was obtained from Aldrich; TMSP and "100%" D_2O were purchased from MSD Isotopes. DCl was obtained from Cambridge Isotopes. Other chemicals and biochemicals were of the highest quality available commercially. pH-stat enzyme activity assays were performed on a Radiometer RTSS Titration System. CD spectra were recorded on a JASCO J-500C spectropolarimeter using a thermostated quartz microcell and processed using DP-500/AT system (version 1.29) software. Proton NMR spectra were recorded on a Bruker AM 500 spectrometer coupled to an Aspect 3000 processing unit.

Construction and Purification of Mutant Enzymes. Site-directed mutants were constructed with an Amersham or USB mutagenesis kit used according to the manufacturer's instructions. The position 22 mutants were constructed from oligonucleotides in which the underscored bases in 5′ CAT AAT TGT AAA TAT CAA 3′ were replaced with ATA, AAT, and AGC for F22Y, F22I, and F22A, respectively. The oligonucleotides used for the construction of the position 106 mutants were 5′ AC TTT TGA ATA ACA AAT 3′ (F106Y), 5′ TTT TGA AAT ACA AAT A 3′ (F106I), and 5′ AC TTT TGA AGC ACA AAT AG 3′ (F106A). Recombinant PLA2 was isolated from the *Escherichia coli* expression host BL21-(DE3)[pLysS], harboring the pTO-propla2 plasmid (Deng et al., 1990). All PLA2 enzymes were purified as described elsewhere (Noel et al., 1991; Dupureur et al., 1992b).

Conformational Stability. The conformational stability of each enzyme, represented by the free energy of unfolding, $\Delta G_d^{H_2O}$, was determined by inducing the reversible denaturation of the enzyme with the denaturant guanidine hydrochloride (GdnHCl) and following the loss of secondary structure with circular dichroism (CD) spectroscopy as

Table I: Free Energies of Denaturation Induced by GdnHCl

enzymes	$\Delta G_d^{H_2O}$ (kcal/mol)[a]	$D_{1/2}$ (M)	m (kcal/mol·M)
WT PLA2	9.5	6.9	1.47
F22Y	11.0 (+1.5)	7.0	1.58
F22I	12.2 (+2.7)	7.0	1.73
F22A	10.0 (+0.5)	6.9	1.46
F106Y	10.1 (+0.6)	6.6	1.53
F106I	11.4 (+1.9)	6.9	1.65
F106A	8.6 (–0.9)	5.9	1.47

[a] The error limit is estimated to be ±0.5 kcal/mol.

previously described (Dupureur et al., 1992b). Measurements were made on enzyme solutions at 0.1 mg/mL, 10 mM sodium borate, and 0.1 mM EDTA, pH 8.0, at 30 °C (Ca^{2+} was omitted since it further stabilizes the enzyme to the extent that a complete denaturation curve cannot be obtained within the solubility limit of GdnHCl).

NMR Analysis. Enzyme (10 mg) was dissolved in 0.5 mL (1.5 mM) of D_2O containing 300 mM NaCl and 50 mM $CaCl_2$ and lyophilized. The residue was then dissolved in 0.5 mL of "100%" D_2O and the pH* adjusted to 4.0 with dilute DCl. Spectra were recorded at 37 °C. Chemical shifts are relative to internal sodium 3-trimethylsilylpropionate-*2,2,3,3-d*$_4$.

Kinetic Analysis. Activities toward micellar and monomeric phosphatidylcholine substrates were conducted using a pH-stat method at 100 mM NaCl, 25 mM $CaCl_2$, 1 mM sodium borate, and 0.1 mM EDTA, pH 8.0, at 45 °C as previously described (Noel et al., 1991). The kinetic constants V_{max} and $K_{m,app}$ were determined from Eadie–Hofstee plots (Atkins & Nimmo, 1975) of v vs v/[S] through the use of linear regression analyses. The k_{cat} was calculated from V_{max} utilizing an enzyme molecular mass of 13 500 Da. Specific activities toward micellar DC_7PC and monomeric DC_6PC were assayed at 5 mM substrate; activities toward monomeric DC_7PC were determined at 0.5 mM substrate. Specific activities toward DC_8PM were determined at 0.5 mM substrate in the presence of 1 mM NaCl and 1 mM $CaCl_2$, pH 8, at 22 °C; under these conditions, pancreatic enzymes form premicellar aggregates with this substrate (Jain & Rogers, 1989). Kinetic analysis of PLA2 in the scooting mode on $DC_{14}PM$ vesicles was carried out at 22 °C and pH 8.0 as described previously using the pH-stat method under first-order (Jain et al., 1986a; Jain & Gelb, 1991; Berg et al., 1991) or zero-order conditions (Berg et al., 1991; Jain et al., 1991b).

Dissociation Constants. (A) Protection Methods. The equilibrium dissociation constants for the dissociation of ligands (calcium, inhibitors, products, and the ether substrate analog DTPM) bound to the active site of PLA2 at the interface or in the aqueous phase were determined by monitoring the rate of alkylation of His-48 by *p*-nitrophenacyl bromide as described elsewhere (Jain et al., 1991a). Briefly, PLA2 (30 μM) was incubated at 22 °C in 50 mM cacodylate buffer, pH 7.5, in the presence of 1.6 mM deoxy-LPC, 0.8 mM *p*-nitrophenacylbromide, and the appropriate ligands. At various time intervals, an aliquot containing typically 0.1–100 pmol of the enzyme was diluted into an appropriate assay mixture (Jain et al., 1991b; Niewenhuizen et al., 1974; Radvanyi et al., 1989). The nonlinear regression of the plot of the residual PLA2 activity as a function of time provided the rate constant for inactivation. The equilibrium dissociation constant under a given set of conditions was calculated from the Scrutton–Utter equation described elsewhere (Jain et al., 1991a).

(B) Spectroscopic Methods. Binding of PLA2 to DTPM vesicles was studied by monitoring the resonance energy transfer from the tryptophan residue (Trp-3) on PLA2 (excitation at 285 nm) to the dansyl probe HDNS present in the vesicles or by directly (excitation at 347 nm) monitoring the fluorescence emission of HDNS without energy transfer (Jain & Vaz, 1987). All measurements were carried out on an SLM 4800S spectrofluorimeter. Solutions contained vesicles of DTPM (0.2 mg) and HDNS (4 μg) in 1.5 mL of 10 mM Tris-HCl and 0.5 mM $CaCl_2$, pH 8.0. The fluorescence of the solution was monitored following addition of increasing amounts of the enzyme. Emission was monitored at 495 nm, and the slit width was 4 nm for emission and excitation. Under certain conditions, it was also possible to obtain values of effective equilibrium constants from measurements of the change in the absorbance at 292 nm

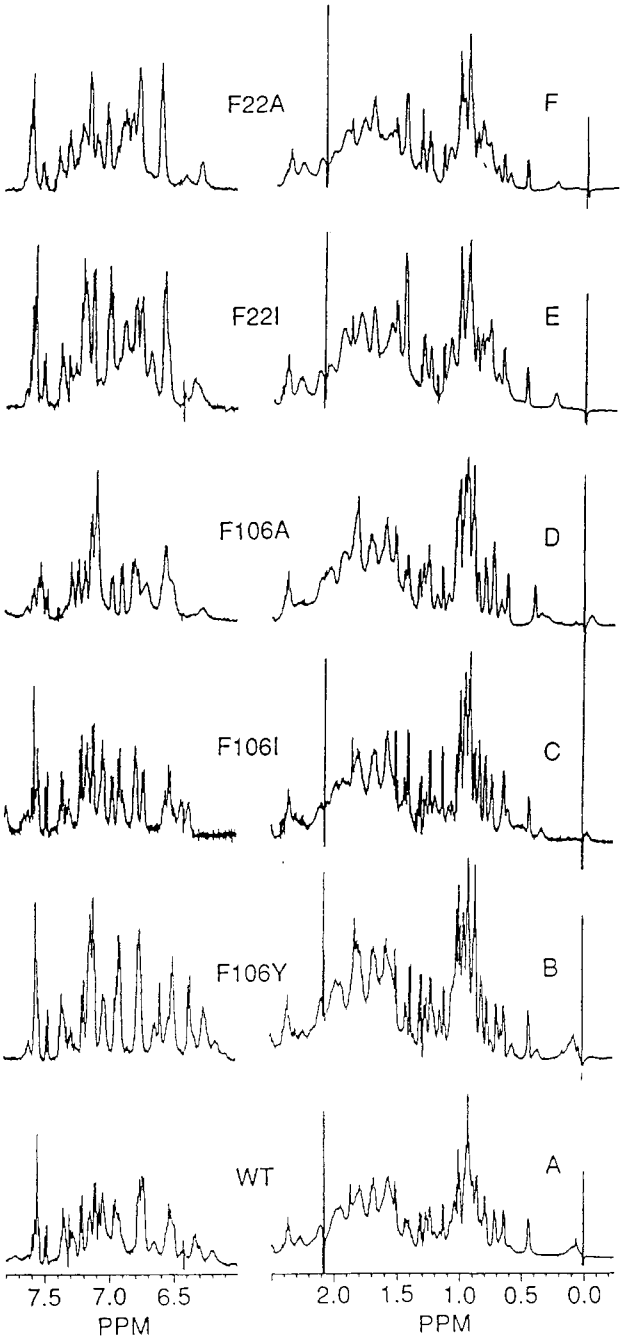

FIGURE 2: One-dimensional proton NMR spectra (500 MHz) of WT (A), F106Y (B), F106I (C), F106A (D), F22I (E), and F22A (F) in D_2O. Sample conditions: 1.5 mM PLA2, 300 mM NaCl, and 50 mM $CaCl_2$, pH* 4.0, at 37 °C. FIDs from 200 scans were processed with Gaussian multiplications (line broadening –5; Gaussian broadening 0.1).

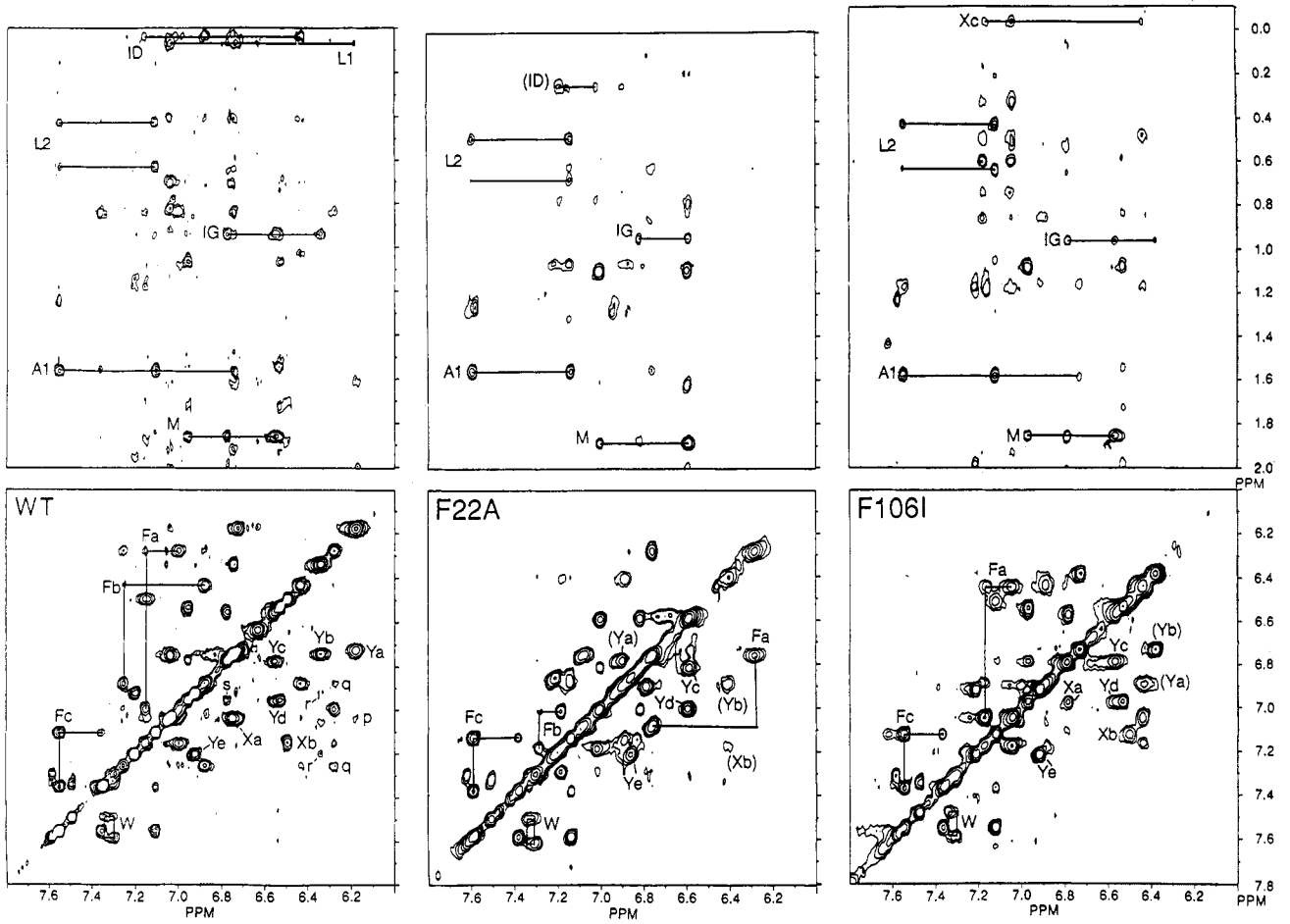

FIGURE 3: Phase-sensitive NOESY spectra of WT, F22A, and F106I in D_2O at 500 MHz. Sample conditions: 1.5 mM PLA2, 300 mM NaCl, and 50 mM $CaCl_2$, pH* 4.0, at 37 °C. The mixing time was 200 ms. A 4096 × 512 matrix in the time domain was recorded and zero-filled to a 4096 × 2048 matrix prior to multiplication by a Gaussian function (line broadening −3; Gaussian broadening 0.1).

(Dupureur et al., 1992b). Similarly, by titrating a mixture of PLA2 and a neutral diluent with a ligand, it was possible to obtain values of effective dissociation constants (Jain et al., to be published).

RESULTS

Conformational Stability. Cooperative reversible unfolding of all mutants was observed upon systematic addition of GdnHCl in an apparent two-state unfolding mechanism. These denaturation data were then analyzed by the standard equation $\Delta G_d = \Delta G_d^{H_2O} - m[\text{GdnHCl}]$, where ΔG_d is the Gibbs free energy change at various concentrations of GdnHCl, $\Delta G_d^{H_2O}$ is that at zero concentration of GdnHCl, and m is a constant related to the susceptibility of the enzyme toward denaturation by the denaturant (Pace, 1986). The $\Delta G_d^{H_2O}$ and m values, along with the midpoint of the denaturation curve ($D_{1/2}$), are listed in Table I. Substitution of either Phe by Tyr, Ile, or Ala did not damage the $\Delta G_d^{H_2O}$ of PLA2 significantly. In fact, the conformational stabilities of F22Y, F22I, and F106I are enhanced by 1.5–2.7 kcal/mol relative to WT. This suggests that despite the fact that Phe-22 and Phe-106 are highly conserved in naturally occurring PLA2 (see Discussion), neither aromaticity nor hydrophobicity at these positions is critically important for conformational stability.

^1H NMR Properties: Qualitative Comparison. One-dimensional ^1H NMR spectra for all mutants except F22Y (a mutant with virtually no change in catalytic activities as described later) are featured in Figure 2. The aromatic regions are predictably different between WT and the mutants. Small but notable differences in the aliphatic region can also be observed. It is therefore necessary to further analyze these spectral characteristics with 2D experiments. NOESY spectra were collected for all five of the mutants; COSY spectra were collected for F106I and F22I to aid in peak assignments for the mutants at each position. Partial NOESY spectra for WT, F22A, and F106I are shown in Figure 3. Qualitatively, similarity of the mutants to WT follows the order WT ≈ F106Y > F106A > F106I ≈ F22A > F22I on the basis of 1D and NOESY spectra.

At first glance, the notable differences in the proton NMR spectra could imply substantial changes in the conformations of the mutants relative to that of WT. However, examination of the X-ray crystal structure reveals that the immediate environment of Phe-22 and Phe-106 is highly aromatic. As depicted in Figure 1, Phe-5 is within 5 Å of these residues. Tyr-111 interacts in an edge-to-face fashion with Phe-22. Thus site-specific substitutions of Phe-22 or Phe-106, particularly by nonaromatic residues, could cause substantial perturbations even if the global conformation is not perturbed. It is therefore important to compare the spectral properties between WT and mutants as quantitatively as possible. This was achieved by comparing the chemical shifts of aromatic spin systems and a few other residues, as described in the following two sections. Since there are a total of 12 Phe, Tyr, and Trp residues spread globally, their chemical shifts can serve as reporters for the perturbation in the global conformation of the mutants.

Table II: Chemical Shifts of the Aromatic Spin Systems for WT and Mutants[a]

spin system	possible assignments	WT			F22A			F106I		
Fa	(F5)	6.28	7.00	7.15	6.28	6.76	7.08	6.45	7.04	7.17
Fb	F106	6.43	6.88	7.26	7.01	7.19	7.28			
Fc	F94	7.10	7.35	7.55	7.15	7.38	7.59	7.12	7.37	7.55
Ya	Y111	6.18	6.72		(6.79)	(6.90)		(6.43)	(6.89)	
Yb	Y52	6.34	6.74		(6.41)	(6.89)		(6.38)	(6.73)	
Yc	Y73	6.55	6.78		6.59	6.82		6.57	6.79	
Yd	Y75	6.52	6.95		6.60	7.01		6.53	6.97	
Ye	Y69	6.92	7.20		6.86	7.21		6.91	7.22	
W	W3	7.30	7.34	7.48	7.31	7.38	7.50	7.30	7.34	7.47
		7.58			7.62			7.58		
Xa	(F22)	6.75	7.04					6.79	6.97	
Xb	(Y28)	6.49	7.15		(6.41)	(7.17)		6.50	7.12	
Xc								(−0.04)		
ID	(I9)	0.05			(0.24)					
L1	(L41)	0.07								
L2	L58	0.63	0.44		0.67	0.47		0.64	0.43	
IG	I95	0.94			0.95			0.96		
A1	(A55)	1.56			1.55			1.58		
M	(M8)	1.86			1.89			1.86		

[a] The underlined are resonances which differ by >0.1 ppm between WT and mutant. Parentheses indicate tentative assignments. The designation of spin systems is according to Fisher et al. (1989).

Partial Resonance Assignments. The chemical shifts of aromatic spin systems and a few aliphatic residues for WT, F22A, and F106I are summarized in Table II. Three sources of information were utilized in our limited partial assignments: the partial assignments reported previously for WT bovine PLA2 (Fisher et al., 1989), the spectra of various mutants obtained in our laboratory [Dupureur et al. (1992b) and unpublished results], and distance relationships revealed by the crystal structure. Since the last criterion depends on the assumption that the solution and the crystal structures are the same, our assignments should be considered tentative until complete assignments can be obtained and solution structures calculated. Such complete assignments and conformational calculation have been achieved for the PLA2 from porcine pancreas (Dekker et al., 1991b), but unfortunately the spectral properties of the bovine and the porcine enzymes are different enough that the assignments of one cannot be applied directly to the other.

The designation of spin systems listed in Table II is based on those described by Fisher et al. (1989). Fb disappears in F106A and F106I, confirming the assignment of this spin system to Phe-106. Xa is tentatively assigned to F22. Fa, which persisted through all the mutants and was perturbed in the aliphatic mutants, is tentatively assigned to F5. Our NOESY spectrum of WT displays NOEs near 0 ppm; these have been named L1 and ID and assigned to Leu-41 and Ile-9 by Fisher et al. (1989). Since these residues are located near F22 and F106, their resonances and the corresponding aromatic/aliphatic NOEs are expectedly affected by the aromatic-to-aliphatic mutations, as shown by the shifts of these cross peaks in the spectra of the mutants.

Four additional aliphatic cross peaks assigned by Fisher and co-workers were located in our WT spectrum and labeled according to their system: L2, assigned to Leu-58, and IG, assigned to Ile-95, are independently confirmed by our COSY data (not shown). M, assigned to Met-8, and A1, assigned to Ala-55, are identifiable in our spectra and are tentatively confirmed. In the crystal structure, these aliphatics are all close to aromatics that are distant from the mutation site (Phe-94, Tyr-73, and Tyr-52) and provide additional information with which to judge global conformational changes due to Phe-22 and Phe-106 substitutions.

^{1}H NMR Properties: Semiquantitative Comparison. The resonances which differ between WT and the mutant by >0.1 ppm are underlined in Table II. There are only two such resonances in F106I: those for F5 and Y111. As shown in Figure 1, both residues are in close proximity to F106. For F22A, there are five residues with >0.1 ppm changes in chemical shifts: F5, F106, Y111, Y52, and I9. The first three are in direct proximity to the mutated residue, and the other two are perturbed by only <0.2 ppm. Thus, in all of the aliphatic mutants characterized, the changes in chemical shifts are confined to residues in the immediate environment of the mutation. The same is true for NOE cross peaks: most of the missing aromatic–aromatic NOEs in the mutants are due to interactions with proximal residues; the NOEs related to the active site aromatics Y52, Y69, and Y73 and the more distal residues W3, Y75, F94, M8, A55, L58, and I95 remain virtually undisturbed in most cases. Thus, NMR results are consistent with the stability study results that these residues appear to make a few global structural contributions.

In summary, the results of structural analysis suggest that changing Phe-22 or Phe-106 to Tyr, Ile, or Ala causes little perturbation in conformation or in conformational stability. The Ile mutants are considerably more stable than WT. In addition to the implications for the structural roles of aromatic pairs (see Discussion), these results permit us to interpret kinetic data directly.

Catalytic Properties. Table III summarizes the activities of all mutant PLA2s toward six substrates: DC_8PC, DC_7PC, and DC_8PM micelles; $DC_{14}PM$ vesicles; and DC_6PC and DC_7PC monomers. Mutations to Ile at either position resulted in only minor perturbations in activity. This suggests that the aromaticity is not important to the function of these two residues. Substitution at either of the two positions with Ala resulted in substantial perturbations in catalytic activity, suggesting that the hydrophobic bulk of both residues is important for catalysis. Substitution with Tyr at position 106 resulted in decreased activity. This result suggests that a possible functional role of the Phe residues is to maintain

Table III: Summary of Kinetic Data for WT and All Mutants

enzyme	$DC_{14}PM$ vesicles v_o (s^{-1})	DC_8PC micelles $k_{cat,app}$ (s^{-1})	DC_8PC micelles $K_{m,app}$ (mM)	DC_8PM micelles[a] (s^{-1})	DC_7PC micelles[b] (s^{-1})	DC_7PC monomers[c] (s^{-1})	DC_6PC monomers[c] (s^{-1})
WT[d]	330 ± 5%	675 ± 5%	1.4 ± 15%	830 ± 10%	74 ± 7%	1.6 ± 15%	1.2 ± 15%
F22Y	460	670	3.6	800	52	1.6	0.8
F22I	500	270	2.6	230	16	0.5	0.45
F22A	30	4	5.2	80	2.0	<0.03	<0.007
F106Y	30	48	5.1	70	4.7	<0.03	<0.007
F106I	155	190	3.7	350	26	0.65	0.13
F106A	50	26	2.4	25	15	0.14	0.20

[a] Specific activity at 0.2 mM substrate; premicellar aggregates are formed under these conditions (Jain & Rogers, 1989). [b] Specific activity (s^{-1}) at 5 mM substrate. [c] Specific activity (s^{-1}) at 0.5 mM substrate. [d] The error limits given are our best estimates for WT. The errors could increase as the rates decrease.

hydrophobicity at the active site. However, the same substitution at position 22 did not result in any loss of activity. The differential behavior of the two residues can be rationalized by noting the orientation of the side chains: Phe-22 points outward facing solvent, whereas Phe-106 points into the active site. The trend for monomeric substrates follows that for aggregated substrates: F22Y, F106I, and F22I are little perturbed; F106A, F22A, and F106Y have significantly lower activities. The effect is most dramatic for the latter two enzymes, for which no appreciable rates for either monomeric substrate could be detected. This is very much in contrast to our previous experience with PLA2: In the characterization of all of our other mutants (some 30 to date), activity toward DC_6PC was always measurable, even for enzymes which had rates toward DC_8PC on the order of 1 s^{-1}. Measurements of monomeric rates with the longer-chained DC_7PC yielded the same results.

Dissecting the Specific Steps of Perturbation by Scooting Mode Kinetics. Although the results in Table III clearly indicate that F22A, F106Y, and F106A have reduced activities, these data cannot be interpreted in terms of specific binding or catalytic steps due to the limitations of the various assay methods discussed previously (Dupureur et al., 1992b). Thus we undertook further analysis of the kinetic parameters obtained in the scooting mode (Berg et al., 1991).[2]

As is the case of Tyr-52 and Tyr-73 mutants (Dupureur et al., 1992b), the "dynamic range" of the variation in activities between WT and the mutants are smaller for the scooting-mode v_o values (turnover number at the maximal substrate concentration, i.e., the mole fraction of substrate = 1) than for the apparent k_{cat} values of DC_8PC micelles. The specific reasons for this difference are unclear since the microscopic rate constants of micellar substrates cannot be measured. Even for the most perturbed mutant F22A, the decrease in v_o is only 10-fold. The overall goal of the kinetic studies is to determine whether this 10-fold decrease in v_o is primarily caused by an increase in K_M* (Michaelis constant at the interface), a decrease in k_{cat} (turnover number under saturating conditions), or both. The study involved the following key steps:

(i) It was first demonstrated that the mutants bind to the interface favorably (i.e., the E to E* step) by monitoring the relative fluorescence of HDNS in DTPM vesicles (Jain & Vaz, 1987). As was the case with WT (Dupureur et al., 1992b), the maximal change is observed when the lipid to enzyme mole ratio approaches 40 for all mutants. These results assured that the scooting mode kinetic theories and protocols developed for the hydrolysis of $DC_{14}PM$ vesicles by WT PLA2 are applicable to the mutants.

(ii) As a control, we have ensured that all mutants have the same N_S values as WT PLA2 within experimental error (±8%), which means that they are all catalytically active as monomeric enzymes and that the observed activities of mutants are not due to contaminating WT PLA2. The fact that only a fraction of the total substrate is hydrolyzed at the end of the first-order progress curve further confirms that under kinetic conditions the enzyme molecules do not exchange between vesicles.

(iii) The equilibrium dissociation constants at the interface, K_{Ca}*, K_S*, K_I*, and K_P*, were then obtained from the halftimes of the alkylation of the active site His-48 at the interface of the neutral diluent, deoxy-LPC, in the absence and the presence of the ligand, as described previously (Jain et al., 1991a). However, the halftimes of alkylation are substantially higher for the mutants[3] (Table IV, first row); the numbers further increase in the presence of ligands. The halftimes for F106Y and F106A in the presence of calcium and ligands were so high (>300 min) that the equilibrium dissociation constants could not be measured by the protection method. Thus some of the dissociation constants were measured independently by titrating a mixture of PLA2 and a neutral diluent with a ligand and monitoring the change in the relative fluorescence intensity of the enzyme. A typical titration curve is shown in Figure 4. The equilibrium dissociation constants determined by the fluorescence method are shown in Table V. The values of dissociation constants obtained by the alkylation and fluorescence methods are within a 50% (or 2-fold) range of each other.

As shown by the results summarized in Tables IV and V, the equilibrium dissociation constants vary between WT and mutants, but only by a small factor (typically within a factor

Table IV: Equilibrium Dissociation Constants of WT and Mutant Enzymes[a]

complexes	WT	F22A	F106I
alkylation halftime (min)	1.5	37	10
E·Ca (mM) (K_{Ca})	0.31	0.31	0.18
E*·Ca (mM) (K_{Ca}*)	0.12	0.26	0.24
E*·deoxy-LPC[b]	>1	0.7	>4
E*Ca·deoxy-LPC[b]	>1	0.6	>1
E*Ca·DTPM[b] (K_S*)	0.02	0.11	0.07
E*Ca·DTPC[b] (K_S*)	>0.5	0.5	>0.5
E*Ca·Prod (of $DC_{14}PM$)[b] (K_P*)	0.025	0.06	0.03
E*Ca·MJ33[b] (K_I*)	0.016	0.035	0.03

[a] Determined by the protection method. The dissociation constant is for dissociation of the last species in the complex shown after the dot. The error limits of the parameters vary depending on how they are derived. However, the accuracy is within ±30% even in the worst circumstance. [b] Units in mole fraction.

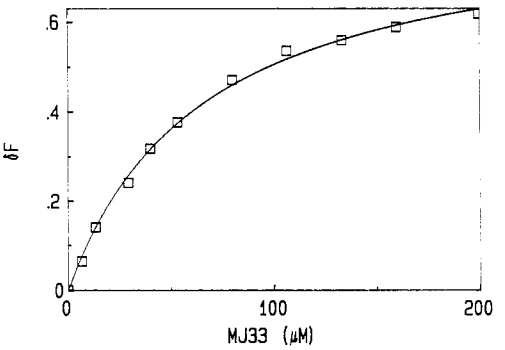

FIGURE 4: Change in the relative fluorescence intensity at 333 nm of F22A (6 μM) in 3.3 mM deoxy-LPC as a function of MJ33. The smooth curve is the rectangular hyperbola obtained by curve fitting to obtain effective dissociation constant, which can be corrected to obtain the K_I* value. Such corrections require the assumption that all the enzyme and inhibitor molecules are at the interface. The evidence for these assumptions has been obtained experimentally, and the results will be presented elsewhere.

[2] Definition of kinetic parameters *at the interface*: K_I*, dissociation constant of inhibitor; K_M*, Michaelis constant; K_P*, dissociation constant of product; K_S*, dissociation constant of substrate; k_{cat}, turnover number at saturating substrate concentration; N_S, the number of phospholipids in the outer monolayer of the vesicle; $N_S k_i$, apparent second-order rate constant; v_o, turnover number at X_S = 1; X_I, mole fraction inhibitor; X_S, mole fraction of substrate. It should be noted that notations K_I*, K_M*, K_P*, and K_S* correspond to K_I, K_{MS}, K_P, and K_S, respectively, used previously (Berg et al., 1991). The revised notations will be used in our future work.

[3] A possible reason for the change in alkylation halftime is a change in the pK_a and/or nucleophilicity of His-48 as a consequence of the change in the hydrophobicity of the active site.

Table V: Equilibrium Dissociation Constants Measured by the Fluorescence Method[a]

complexes	WT	F22A	F106I	F106A	F106Y
K_P* ($DC_{14}PM$)	0.02	0.03	0.015	0.07	0.04
K_I* (MJ33)	0.009	0.031	0.02	0.18	0.02

[a] The error limits are generally ±10%. Units in mole fraction.

Table VI: Catalytic Parameters for the Hydrolysis of $DC_{14}PM$ by WT and Mutants

parameter	WT	F22A	F106Y	F106A	F106I
v_o (s^{-1})	330	30	45	105	155
$X_I(50)$ (mol fraction)	0.055	0.11	0.08	0.28	0.06
K_M* (mol fraction)	0.60	0.25	0.26	0.45	0.67
k_{cat} (s^{-1})	530	37	57	150	260
k_{cat}/K_M* [a]	880	148	220	330	390
$N_S k_i$ (s^{-1})	30	11	12	10	24
k_{cat}/K_M* [b]	1230	200			910

[a] Calculated from eqs 1 and 2. [b] Calculated from eq 3.

of 3). These results suggest that the binding properties at the interface (E* to E*L) are similar between WT and mutants.

(iv) Two approaches were undertaken to determine the catalytic parameters at the interface (i.e., K_M*, k_{cat}, and/or k_{cat}/K_M*). (a) The experimentally measured v_0 value is related to k_{cat} and K_M* according to the following equation:

$$v_o = k_{cat}/(1 + K_M^*) \quad (1)$$

The interfacial Michaelis constant K_M* was calculated from initial rates of hydrolysis of $DC_{14}PM$ in the absence and presence of the competitive inhibitor MJ33 [$(v_o)^o$ and $(v_o)^I$, respectively] according to the following equation (Berg et al., 1991; Jain et al., 1991a):

$$(v_o)^o/(v_o)^I = 1 + [(1 + 1/K_I^*)/(1 + 1/K_M^*)] \times [X_I/(1 - X_I)] \quad (2)$$

where X_I is the mole fraction of the inhibitor in the interface, and K_I* is the interfacial dissociation constant of the inhibitor. The $X_I(50)$ values were then determined from eq 2, and the data are listed in Table VI (row 2). The 2–5-fold increases in the $X_I(50)$ values of mutants (relative to that of WT) are consistent with the relative K_S*, K_P*, and K_I* values. The K_M* values (row 3, Table VI) calculated from eq 2 are similar between WT and mutants. The k_{cat} values calculated from the v_o and K_M* values according to eq 1 (row 4, Table VI) indicate that *the main difference between WT and the mutants lies in k_{cat}*. The decrease is the largest for F22A (13-fold). The same trend is observed for k_{cat}/K_M* (row 5).

(b) The ratio k_{cat}/K_M* can be derived from two other experimentally determined parameters, $N_S k_i$ (the apparent second-order rate constant, obtained from the progress curve of the reaction) and K_P* (the product inhibition constant), according to another key equation:

$$N_S k_i = (k_{cat}/K_M^*)[1/(1 + 1/K_P^*)] \quad (3)$$

The values thus obtained (last row, Table VI) are somewhat higher than the values obtained from eq 1, but the relative values between WT and mutants agree very well between the two approaches.

DISCUSSION

We have undertaken a multifaceted study which probes the structure–function relationships of Phe-22 and Phe-106 in PLA2. Both residues are highly conserved. The existence of Tyr at position 22 for a few natural variants has been known for some time (Botes & Viljoen, 1974; Halpert & Eaker, 1975, 1976; Heinrickson et al., 1977). For such variants, the phenolic hydroxyl of residue 22 would point toward solvent and as such would likely have little impact on the character of the active site. Our kinetic and stability data for F22Y clarify why this substitution is well-tolerated among natural variants. To our knowledge, there are no other known natural substitutions of Phe-22. The hydrophobicity of residue 106, in which the ring points into the active site, appears to be more invariant. Like position 22, aromaticity is highly conserved, although a few newly sequenced PLA2s actually have Leu at position 106 (Davidson & Dennis, 1990). The data indicating that F106I is only marginally perturbed in both structure and function are consistent with this natural variety.

Lack of Structural Roles for Aromatic Pairs. It has been demonstrated that edge-to-face geometry among aromatic pairs can contribute 1.5 kcal/mol of stabilization energy to a protein (Burley & Petsko, 1988; Serrano et al., 1991). On the other hand, face-to-face aromatic stacking like that seen for Phe-22 and Phe-106 is less common in proteins (constituting only 7% of all aromatic pairs) and, according to energy calculations, is theoretically expected to contribute very little stabilization energy (Singh & Thornton, 1985; Burley & Petsko, 1985). Although the $\Delta G_d^{H_2O}$ value is only one of several ways to measure stability, our results provide the first experimental evidence to support the theoretical prediction that a face-to-face aromatic pair contributes little to conformational stability. In fact, the conformational stabilities of the Ile mutants are actually enhanced by as much as 2.7 kcal/mol. Although such increases in conformational stability could be caused by favorable interactions between the new Ile side chain and the side chains of the neighboring Ile-9 and Leu-41 (Figure 1B), they cannot be rationalized simply by relative hydrophobicities (which are the same for Ile and Phe side chains).

On the other hand, the prediction that an edge-to-face arrangement is energetically important is not supported by our studies of Phe-22, which forms an edge-to-face pair with Tyr-111. The lack of contribution to conformational stability by edge-to-face aromatic pairs has also been observed for the Tyr-52/Tyr-69 pair and the Tyr-73/Tyr-75 pair (Dupureur et al., 1992b). Proton NMR results provide more detailed information that corroborates the stability results: all Phe-22 and Phe-106 mutants are indeed quite structurally similar to wild type. *These results establish that the conserved residues Phe-22 and Phe-106 do not have structural roles.*

Large, Apolar Side Chains at Positions 22 and 106 Are Important to Activity. The activities of F106Y, which introduces hydrophilicity, and F22A and F106A, which have hydrophobic but small side chains, are low relative to WT. These results are consistent with a requirement for side chains which are both large and apolar. Such residues could contribute to catalysis in two possible ways: (i) As mentioned in the introduction, the side chains of Phe-22 and Phe-106 could be important to substrate binding by aligning *sn*-2 acyl chain. This possibility is supported by structural data on enzyme–inhibitor complexes (White et al., 1990; Scott et al., 1990; Thunnissen et al., 1990; Dekker et al., 1991). Our results, however, go beyond the structural information by revealing that the contribution of such alignment to catalysis is relatively modest and lies primarily in k_{cat} and k_{cat}/K_M*. (ii) Hydrophobic bulk at these positions could also be involved in maintaining the hydrophobicity of the active site. The remarkable conservation of the hydrophobic wall and the remarkably dehydrated state of the active site (van Schar-

renburg et al., 1985) is consistent with this hypothesis. When the hydrophobicity is not optimal as in F22A, F106A, and F106Y, catalysis is perturbed. Indeed, the behavior of the semisynthetic mutant F5Y (van Scharrenburg et al., 1982), in which the new tyrosyl side chain points in the same direction as Tyr-106, is similar to that of F106Y.

While our data are sufficient to pinpoint k_{cat} as the primary parameter of perturbation in the interfacial catalysis by F22 and F106 mutants, the magnitudes of the overall effects are not sufficient for further dissection. The data in Tables IV and V show that the dissociation constants for substrate, product, and inhibitor are also perturbed, but to a smaller extent. On the other hand, the K_M* values of the mutants decrease relative to WT. Considering the relatively large range of errors for lipid substrates (generally ±30%), the data should not be overinterpreted. It is difficult to attribute a factor of 10 in overall activity to microscopic rate constants even in a well-established and well-defined assay system.

Conclusion. Recent major developments in structural studies (White et al., 1990; Thunnissen et al., 1990; Dekker et al., 1991) and kinetic analysis (Jain & Berg, 1989; Berg et al., 1991) of PLA2 have provided a basis for integrated structure–function studies of interfacial catalysis such as the work described in this paper. The results of structural analysis indicate that disrupting the Phe-22/Phe-106 aromatic face-to-face pair or the Phe-22/Tyr-111 edge-to-face pair does not lead to notable perturbations in the conformation or conformational stability of PLA2. The results of functional studies suggest that bulky hydrophobic side chains at positions 22 and 106 are required for optimal catalytic activity, possibly by aligning the 2-acyl chain as suggested by structural analysis and/or by maintaining hydrophobicity at the active site.

ACKNOWLEDGMENT

We are indebted to Xiaoyan Zhang and Yuan Ji for assistance in enzyme purification.

REFERENCES

Atkins, G. L., & Nimmo, I. A. (1975) *Biochem. J. 149*, 775–779.
Berg, O. G., Yu, B.-Z., Rogers, J., & Jain, M. K. (1991) *Biochemistry 30*, 7283–7297.
Botes, D. P., & Viljoen, C. C. (1974) *J. Biol. Chem. 249*, 3827–3835.
Burley, S. K., & Petsko, G. A. (1985) *Science 229*, 23–28.
Burley, S. K., & Petsko, G. A. (1988) *Adv. Protein Chem. 39*, 125–189.
Davidson, F. F., & Dennis, E. A. (1990) *J. Mol. Evol. 31*, 228–238.
Dekker, N., Peters, A. R., Slotboom, A. J., Boelens, R., Kaptein, R., Dijkman, R., & de Haas, G. H. (1991a) *Eur. J. Biochem. 199*, 601–607.
Dekker, N., Peters, A. R., Slotboom, A. J., Boelens, R., Kaptein, R., & de Haas, G. H. (1991b) *Biochemistry 30*, 3135–3147.
Deng, T., Noel, J. P., & Tsai, M.-D. (1990) *Gene 93*, 229–234.
Dijkstra, B. W., Kalk, K. H., Hol, W. G. J., & Drenth, J. (1981a) *J. Mol. Biol. 147*, 97–123.
Dijkstra, B. W., Drenth, J., & Kalk, K. H. (1981b) *Nature 289*, 604–606.
Dupureur, C. M., Li, Y., & Tsai, M.-D. (1992a) *J. Am. Chem. Soc. 114*, 2748–2749.
Dupureur, C. M., Yu, B.-Z., Jain, M. K., Noel, J. P., Deng, T., Li, Y., Byeon, I.-J. L., & Tsai, M.-D. (1992b) *Biochemistry 31*, 6402–6413.
Fisher, J., Primrose, W. U., Roberts, G. C. K., Dekker, N., Boelens, R., Kaptein, R., & Slotboom, A. J. (1989) *Biochemistry 28*, 5939–5946.
Heinrickson, R. L., Krueger, E. T., & Keim, P. S. (1977) *J. Biol. Chem. 252*, 4913–4921.
Halpert, J., & Eaker, D. (1975) *J. Biol. Chem. 250*, 6990–6997.
Halpert, J., & Eaker, D. (1975) *J. Biol. Chem. 251*, 7343–7347.
Jain, M. K., & Berg, O. G. (1989) *Biochim. Biophys. Acta 1002*, 127–156.
Jain, M. K., & Rogers, J. (1989) *Biochim. Biophys. Acta 1003*, 91–97.
Jain, M. K., & Vaz, W. L. C. (1987) *Biochim. Biophys. Acta 906*, 1–8.
Jain, M. K., & Gelb, M. H. (1991) *Methods Enzymol. 197*, 112–125.
Jain, M. K., Rogers, J., Jahagirdar, D. V., Marecek, J. F., & Ramirez, F. (1986) *Biochim. Biophys. Acta 860*, 435–447.
Jain, M. K., Yu, B.-Z., Rogers, J. Ranadive, G. N., & Berg, O. G. (1991a) *Biochemistry 30*, 7306–7317.
Jain, M. K., Rogers, J., Berg, O. G., & Gelb, M. H. (1991b) *Biochemistry 30*, 7340–7348.
Jain, M. K., Tao, W., Rogers, J., Arenson, C., Eibl, H., & Yu, B.-Z. (1991c) *Biochemistry 30*, 10256–10268.
Jain, M. K., Tao, W., Rogers, J., Arenson, C., Eibl, H., & Yu, B.-Z. (1991d) *Biochemistry 30*, 10256–10268.
Nieuwenhuizen, W., Kunze, H., & de Haas, G. H. (1974) *Methods Enzymol. 32B*, 147–154.
Noel, J. P., Bingman, C., Deng, T., Dupureur, C. M., Hamilton, K. J., Jiang, R.-T., Kwak, J.-G., Sekharudu, C., Sundaralingam, M., & Tsai, M.-D. (1991) *Biochemistry 30*, 11801–11811.
Pace, C. N. (1986) *Methods Enzymol. 131*, 266–279.
Randvanyi, F., Jordan, L., Russo-Marie, F., & Bon, C. (1989) *Anal. Biochem. 177*, 103–109.
Rosario-Jansen, T., Pownall, H. J., Noel, J. P., & Tsai, M.-D. (1987) *Phosphorus Sulfur Relat. Elem. 30*, 601–604.
Scott, D. L., Otwinowski, Z., Gelb, M. H., & Sigler, P. B. (1990) *Science 250*, 1563–1566.
Sekharudu, C., Ramakrishnan, B., Huang, B., Jiang, R.-T., Dupureur, C. M., Tsai, M.-D., & Sundaralingam, M. (1992) *Protein Sci.* (in press).
Serrano, L., Bycroft, M., & Fersht, A. R. (1991) *J. Mol. Biol. 218*, 465–475.
Singh, J., & Thornton, J. M. (1985) *FEBS Lett. 191*, 1–6.
Thunnissen, M. M. G. M., Ab, E., Kalk, K. H., Drenth, J., Dijkstra, B. W., Kuipers, O. P., Dijkman, R., de Haas, G. H., & Verheij, H. M. (1990) *Nature 347*, 689–691.
van Scharrenberg, G. J. M., Puijk, W. C., Egmond, M.R., van der Schaft, P. H., de Haas, G. H., & Slotboom, A. J. (1982) *Biochemistry 21*, 1345–1352.
van Scharrenburg, G. J. M., Slotboom, A. J., de Haas, G. H., Mulqueen, P., Breen, P. J., & Horrocks, W. DeW., Jr. (1985) *Biochemistry 24*, 334–339.
White, S. P., Scott, D. L., Otwinowski, Z., Gelb, M. H., & Sigler, P. (1990) *Science 250*, 1560–1563.